© 2014. Published by The Company of Biologists Ltd | Development (2014) 141, 2978-2983 doi:10.1242/dev.109694

RESEARCH REPORT

The F-box protein Slmb restricts the activity of aPKC to polarize epithelial cells

Lara C. Skwarek[1], Sarah L. Windler[1], Geert de Vreede[1], Gregory C. Rogers[2] and David Bilder[1,*]

ABSTRACT

The Par-3/Par-6/aPKC complex is the primary determinant of apical polarity in epithelia across animal species, but how the activity of this complex is restricted to allow polarization of the basolateral domain is less well understood. In *Drosophila*, several multiprotein modules antagonize the Par complex through a variety of means. Here we identify a new mechanism involving regulated protein degradation. Strong mutations in *supernumerary limbs* (*slmb*), which encodes the substrate adaptor of an SCF-class E3 ubiquitin ligase, cause dramatic loss of polarity in imaginal discs accompanied by tumorous proliferation defects. Slmb function is required to restrain apical aPKC activity in a manner that is independent of endolysosomal trafficking and parallel to the Scribble module of junctional scaffolding proteins. The involvement of the Slmb E3 ligase in epithelial polarity, specifically limiting Par complex activity to distinguish the basolateral domain, points to parallels with polarization of the *C. elegans* zygote.

KEY WORDS: *Drosophila*, Par, Epithelia, Polarity, Tumor, Ubiquitin ligase

INTRODUCTION

Polarization is a fundamental feature of animal cells, from newly fertilized zygotes to dividing stem cells to homeostatic epithelia. This common feature is controlled by a conserved set of regulators, which segregate the single plasma membrane into several discrete domains. The most broadly used polarity regulators comprise the Par complex, consisting of the PDZ-containing scaffolds Par-3 and Par-6, which associate with Cdc42-GTP and the atypical protein kinase (aPKC) (Goldstein and Macara, 2007; St Johnston and Ahringer, 2010). In the *C. elegans* zygote and the *Drosophila* oocyte, these proteins localize to and specify the anterior cortex. In most epithelial cells and neural stem cells, they localize to and specify the apical plasma membrane, and in migrating cells they define and act at the leading edge. The Par complex thus serves as a 'master regulator' for many types of cell polarity.

To achieve and maintain polarity, the Par complex must be restrained to distinguish a complementary membrane domain. In contrast to the pre-eminent role of the Par complex, multiple protein modules that limit Par activity have been identified in different contexts (Tepass, 2012). In the *C. elegans* zygote, the protein kinases PAR-1 and PAR-4 act downstream of the RING finger protein PAR-2 to antagonize Par localization and define the posterior cortex (St Johnston and Ahringer, 2010; Zonies et al., 2010). Par-1 and Par-4 (Lkb1 – FlyBase) are also key regulators of fly oocyte polarization, but often have less central roles in other polarized cell types (Haack et al., 2013; Partanen et al., 2013). Instead, in many of these tissues a second group of proteins, the Scribble (Scrib) module, acts to restrict the Par complex. In the Scrib module, Scrib and Dlg are basolaterally localized PDZ-containing scaffolds that regulate Lgl, a syntaxin- and myosin-binding protein that can directly antagonize aPKC (Bilder, 2004; Elsum et al., 2012). Yet another module, the Yurt/Coracle (Cor) complex, specifies the basolateral domain in mid-stage *Drosophila* embryos and zebrafish photoreceptors (Laprise and Tepass, 2011). Rac and PI3 kinase also play a role at this stage (Chartier et al., 2011). Further, in fly epithelia but not neuroblasts, AP-2-mediated endocytosis restricts apical polarity regulators to their appropriate surface; endocytosis also plays a crucial role in polarization of the worm zygote (Halbsgut et al., 2011; Shivas et al., 2010). The mechanisms by which this diverse set of proteins – which we will call Par or apical antagonists – negatively regulate the Par complex is an active field of investigation. In none of these cases is the mechanism well understood, nor how they coordinate with each other.

Our incomplete knowledge of the mechanisms of Par antagonists raises the possibility that additional regulators of basolateral polarity remain to be identified. Here we report that strong mutations in the F-box protein Slmb, a substrate adaptor for SCF E3 ubiquitin ligases, result in excess Par complex activity in *Drosophila* imaginal discs, thereby expanding the apical membrane domain. Our results indicate that Slmb-mediated protein degradation acts in parallel to the Scrib module to oppose aPKC activity and thus specify the epithelial basolateral membrane.

RESULTS AND DISCUSSION

Slmb is a novel *Drosophila* neoplastic tumor suppressor gene

To identify new regulators of basolateral polarity, we analyzed mutants isolated in a genetic screen for *Drosophila* tumor suppressor genes (TSGs). The screen utilized mitotic recombination to generate imaginal discs predominantly populated by homozygous mutant cells growing in an otherwise heterozygous larva. Mutations in a small set of genes cause larval or pupal lethality in this context; many of these show a set of tumor-like phenotypes collectively called 'neoplastic' (Menut et al., 2007). Discs mutant for one uncharacterized complementation group, *MENE(3R)-B*, show multiple hallmarks of neoplastic transformation. Monolayered organization is lost, disc size is dysregulated, F-actin levels are elevated and differentiation is prevented (Fig. 1A-F). In addition, Matrix metalloproteinase 1 (Mmp1), a mediator of tissue invasion, is upregulated (Fig. 1A,B). These phenotypes closely resemble those of the Scrib module, suggesting that *MENE(3R)-B* identifies a gene with similar function.

MENE(3R)-B alleles fail to complement mutants in *slmb*, which encodes an F-box and WD40 repeat protein homologous to vertebrate β-TrCP (Btrc) that functions as a specificity factor in a Skp–Cullin–F-box (SCF) E3 ubiquitin ligase complex (Frescas and Pagano, 2008;

[1]Department of Molecular and Cell Biology, University of California Berkeley, Berkeley, CA 94720-3200, USA. [2]Department of Cellular and Molecular Medicine, University of Arizona Cancer Center, University of Arizona, Tucson, AZ 85724, USA.

*Author for correspondence (bilder@berkeley.edu)

Received 5 March 2014; Accepted 2 June 2014

Development (2014) 141, 2978-2983 doi:10.1242/dev.109694

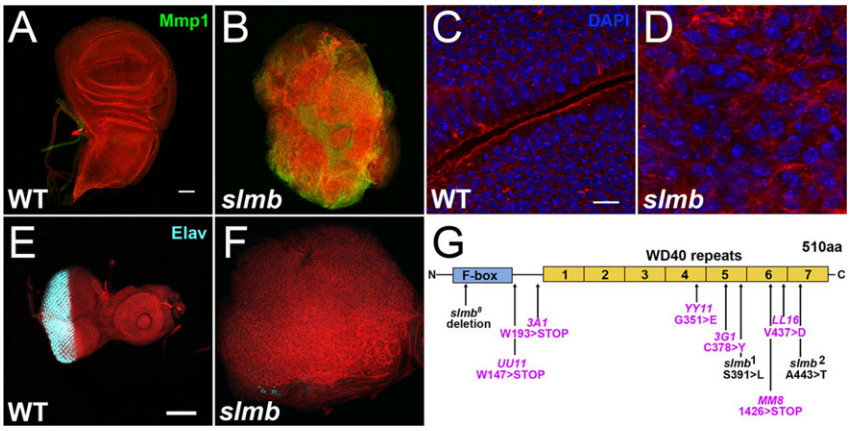

Fig. 1. *slmb* is a novel neoplastic tumor suppressor gene. (A-D) *slmb* wing discs show upregulation of Mmp1 (green) and loss of epithelial organization. DNA (DAPI), blue; F-actin (Phalloidin stain) is red in all figures. (E,F) *slmb* eye discs fail to differentiate. Elav, cyan. (G) Domain structure of Slmb and identified lesions. *MENE(3R)-B* alleles in violet text. Scale bars: 50 μm in A,E; 10 μm in C.

Jiang and Struhl, 1998; Theodosiou et al., 1998). Sequencing identified coding region lesions, including early and late truncations as well as missense mutations, in all six alleles (Fig. 1G), and a *slmb* transgene rescues the neoplastic phenotype (supplementary material Fig. S1). The existing alleles $slmb^{1}$ and $slmb^{2}$ have been widely used, and epithelial organization phenotypes have not been reported. Sequencing revealed that these contain missense mutations in the fifth and seventh WD40 domains (Fig. 1G), indicating that both may be hypomorphic. We confirmed that $slmb^{1}$ and $slmb^{2}$ mutant discs show no and only a limited degree of neoplastic transformation, respectively (supplementary material Fig. S1). However, discs predominantly mutant for the deletion allele $slmb^{8}$ (Milétich and Limbourg-Bouchon, 2000) show neoplasia, confirming that this phenotype is induced only by strong alleles. Null mutations in *Roc1a*, which encodes a frequent component of the SCF^{Slmb} complex (Noureddine et al., 2002), also show neoplasia (supplementary material Fig. S1). These data demonstrate that *slmb* functions as a new neoplastic TSG, and suggest that it does so via its role in the SCF^{Slmb} E3 ligase.

Slmb restricts apical polarity

Known neoplastic TSGs regulate epithelial polarity. We therefore analyzed *slmb* tissue with markers for polarized membrane domains. In wild-type (WT) imaginal epithelia, the transmembrane proteins Cadherin 87 (Cad87) and Fasciclin III (FasIII) occupy complementary apical and basolateral membrane domains. In *slmb* cells, Cad87 is distributed ectopically around the cell circumference in discontinuous domains that sometimes overlap with FasIII (Fig. 2A,B). Similar effects are seen with the polarized peripheral membrane proteins Bazooka (Baz; *Drosophila* Par-3) and Cor (Fig. 2C,D). Expanded apical domains of *slmb* tissue resemble those of Scrib module mutants (Fig. 2E), and indicate that Slmb also acts as an apical antagonist.

To explore the breadth of Slmb function in cell polarity, we attempted to generate clones of strong alleles in other tissues. We were generally unable to recover clones in the follicle cell epithelium, and females carrying germline clones failed to produce eggs, preventing analysis of embryonic epithelia (data not shown). Clones in the larval central nervous system showed defective optic lobe organization. Intriguingly, clones derived from type I neuroblasts frequently contained multiple neuroblast-like cells, suggesting that Slmb might also be required for asymmetric cell division (supplementary material Fig. S2) (Li et al., 2014).

Slmb does not regulate endolysosomal trafficking

Of the known Par antagonists, only the Scrib module and endocytic components have been shown to strongly regulate imaginal basolateral polarity, raising the possibility that *slmb* might act primarily via one of these pathways. We first asked whether either Scrib or endocytic components promote Slmb-mediated protein degradation. However, Armadillo (Arm) levels (Jiang and Struhl, 1998) are not increased in *scrib* or *AP-2σ* depleted tissue (Fig. 3A-C), nor was there evidence for misregulation of other Slmb targets

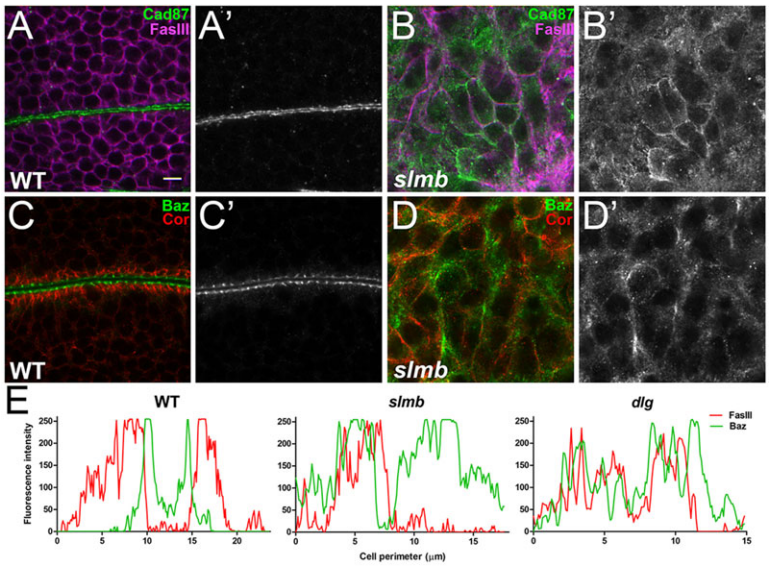

Fig. 2. Slmb represses apical polarity. (A-D′) WT and *slmb* wing discs stained for the transmembrane proteins Cad87 (apical, green) and FasIII (basolateral, magenta) (A,B) or peripheral proteins Baz (apical, green) and Cor (basolateral, red) (C,D). In the absence of Slmb, distinct domains are lost and apical proteins expand around the cell cortex. A′-D′ show single-channel images of apical markers. (E) Quantitation of Baz and FasIII staining along plasma membrane profiles of representative WT, *slmb* and *dlg* cells documents apical expansion. The *x*-axis is the length along the cell perimeter; 0 is the arbitrary spot where the measurement began. Scale bar: 5 μm.

Development (2014) 141, 2978-2983 doi:10.1242/dev.109694

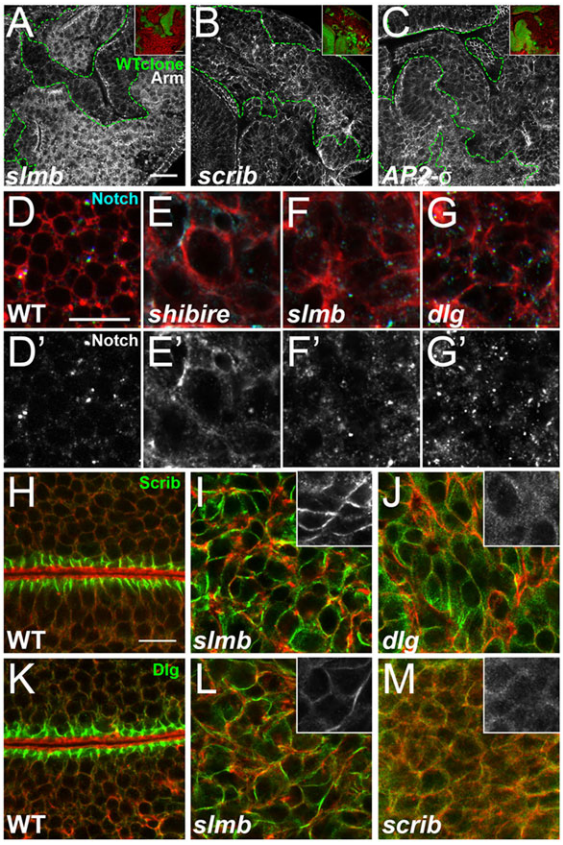

Fig. 3. Slmb is not a regulator of endolysosomal traffic and acts in parallel to the Scrib module. (A-C) *slmb* cells exhibit increased Arm, whereas *dlg* and *AP-2σ* cells do not. Inset shows clonal boundaries. (D-G′) Wing discs cultured with lysosomal inhibitor and stained for Notch. Notch is trapped prior to the lysosomal accumulation in *shibire* tissue, but in *slmb* or *dlg* tissue is trafficked similar to in WT. D′-G′ show Notch (cyan) and F-actin (red) staining. (H-M) Scrib and Dlg remain cortical in *slmb* mutants, but are lost from the plasma membrane in *dlg* or *scrib* mutants. Insets show higher magnification of Scrib (I) or Dlg (L) localization. Scale bars: 25 μm in A; 10 μm in D,H.

(supplementary material Fig. S3). We next asked whether Slmb might act through either the Scrib module or endocytic regulators to restrain apical polarity. To test whether Slmb interferes with AP-2-mediated endocytosis, we analyzed Notch trafficking and used a lysosomal inhibitor to monitor accumulation in the endolysosomal pathway (Windler and Bilder, 2010). Endocytic mutants prevent this accumulation (Fig. 3E), but in *slmb*, as in WT and Scrib module mutant discs, Notch is internalized and trafficked appropriately to endolysosomal compartments (Fig. 3D,F,G). Consistent with a lack of involvement in endocytic regulation, heterozygosity for *slmb* does not enhance a weak *avalanche* (*Syntaxin 7*) *RNAi* phenotype, which is sensitive to the dosage of endocytic regulators of polarity (Morrison et al., 2008). Taken together, these data fail to support a general endocytic role for Slmb.

Slmb and Scrib regulate polarity via distinct but parallel pathways

To test whether Slmb might directly influence Scrib module activity, we examined protein localization. A distinctive feature of *scrib* and *dlg* mutants is that, although many proteins are mispolarized, Dlg is specifically lost from the plasma membrane of *scrib* mutants, as is Scrib in *dlg* mutants (Bilder et al., 2000). By contrast, examination of *slmb* mutant cells reveals that both Scrib and Dlg retain tight, albeit dysregulated, cortical localization (Fig. 3H-M). Additionally, heterozygosity for *slmb* does not enhance weak *lgl-RNAi* nor *lgl* or *dlg* hypomorphic phenotypes, all of which are sensitive to the dosage of Scrib module components (H. A. Morrison and B. D. Bunker, PhD theses, University of California Berkeley, 2010). Thus, despite the many phenotypic similarities, the failure to control Scrib and Dlg membrane recruitment and the lack of genetic interaction suggest that Slmb regulates polarity in parallel to the Scrib module.

Misregulation of known substrates cannot account for the *slmb* null phenotype

The strong neoplastic phenotype seen in *slmb* tissue points to the existence of a polarity-regulating substrate, the levels of which must be controlled. We therefore examined known Slmb substrates to see whether any could account for this phenotype (supplementary material Fig. S4). Both Arm and Cubitus interruptus (Ci) are subject to proteolytic regulation by Slmb. Cells individually expressing or co-expressing active, non-degradable forms of Arm and Ci display a degree of hyperplastic overgrowth, consistent with known roles in the imaginal disc, but retain normal polarity and tissue architecture and do not upregulate Mmp1 (supplementary material Fig. S4A). Overexpression of stabilized Plk4 (Sak kinase – FlyBase) and Cap-H2 (Buster et al., 2013; Rogers et al., 2009) caused no growth or polarity phenotypes (supplementary material Fig. S4B,C). Overexpression of a stabilized form of the polarity kinase Par-1, recently shown to be an Slmb substrate at *Drosophila* synapses (Lee et al., 2012), also failed to phenocopy *slmb* loss. This suggests that an unidentified Slmb substrate normally regulates epithelial organization in imaginal discs.

aPKC is required for *slmb*-mediated neoplastic transformation

An attractive candidate target of Slmb-mediated polarity regulation is the Par complex component aPKC. Overexpression of activated aPKC is sufficient to expand the apical domain and confer neoplastic phenotypes similar to those of *slmb* tissue (Fig. 4O) (Eder et al., 2005). Intriguingly, one predicted isoform of aPKC (aPKC-G) contains two Slmb-binding degrons and, when expressed in S2 cells, is degraded in an *slmb*-dependent manner (supplementary material Fig. S4). However, *aPKC-G* transcripts are present at very low levels in L3 discs, and expression of a degron-lacking aPKC-G had no effect on disc polarity or growth (supplementary material Fig. S4). We then used an antibody directed against a shared protein region to analyze total aPKC and found that it is mispolarized in *slmb* tissue and more widely distributed around the plasma membrane (Fig. 4A,B). However, aPKC levels are not obviously elevated, as assessed by immunohistochemistry, when compared with neighboring WT cells, in contrast to the evident elevation seen with Arm (Fig. 3A). We quantitated western blots of disc lysates which indicated a modest but not significant elevation of aPKC in *slmb* versus WT (Fig. 4C). These data suggest that, although aPKC is mislocalized in *slmb* cells, it is unlikely to be a target of *slmb*-mediated degradation.

Despite the absence of elevated levels of aPKC, we found multiple signs of increased aPKC activity in *slmb* discs. Excessive aPKC activity drives neoplastic overgrowth in part through upregulation of JAK-STAT pathway ligands, mediated by the Yorkie (Yki) transcription factor (Doggett et al., 2011; Robinson and Moberg, 2011; Sun and Irvine, 2011). *slmb* discs show robust activation of a STAT signaling reporter, and their neoplastic phenotype is sensitive to the dosage of *yki* (Fig. 4D-G). A second aPKC-regulated process is seen upon overexpression of the Crb intracellular domain in photoreceptors (Fig. 4H,I) (Tanentzapf and

Development (2014) 141, 2978-2983 doi:10.1242/dev.109694

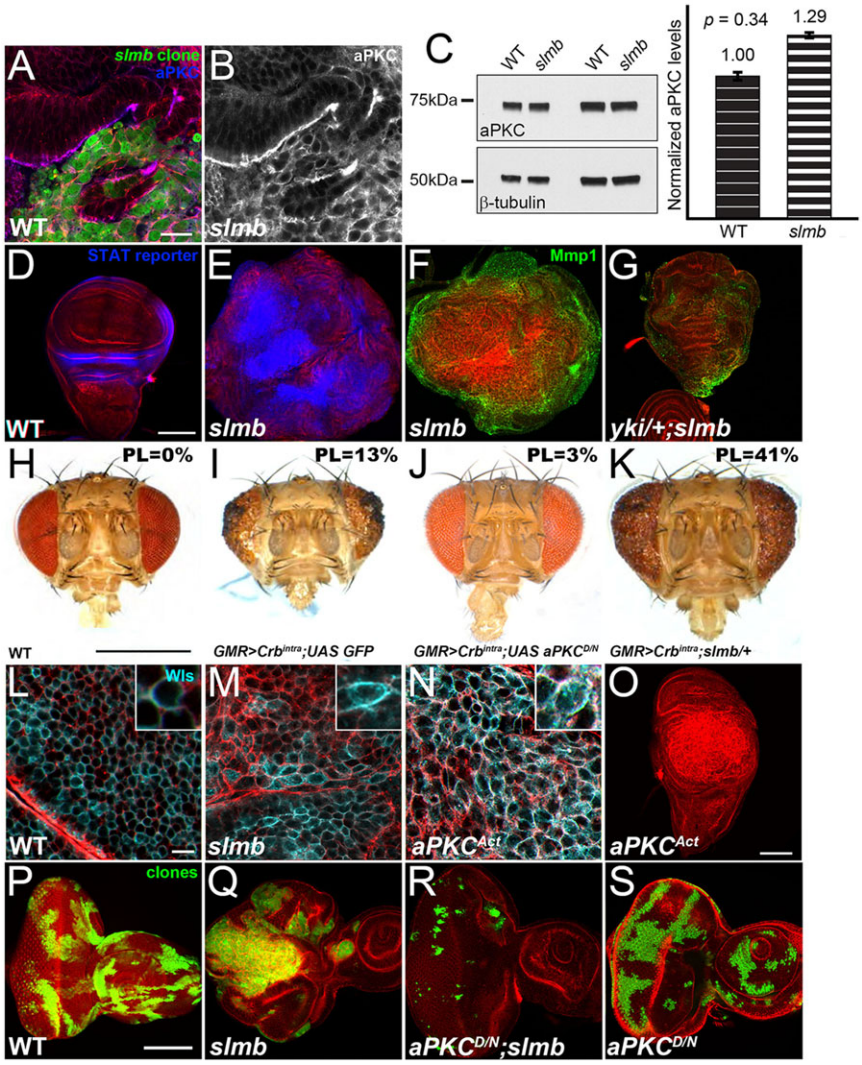

Fig. 4. Slmb limits aPKC activity to prevent neoplasia. (A,B) aPKC localization is expanded in *slmb* cells. (C) Western blots of WT and *slmb* wing discs. aPKC levels are normalized to β-tubulin and quantitated. Error bars indicate s.e. (D,E) A JAK/STAT pathway reporter (blue) is elevated in *slmb*. (F,G) The *slmb* neoplastic phenotype is sensitive to levels of *yki*. (H-K) Crb^{intra} expression in developing photoreceptors causes eye defects. This phenotype reflects excess aPKC activity and is enhanced by loss of one copy of *slmb*. PL, degree of pupal lethality. (L-N) Wntless (Wls, cyan) is cortical in WT cells but accumulates subcortically in *slmb* mutant and activated aPKC-expressing cells. (O) Neoplastic transformation driven by excess aPKC activity in the wing pouch. (P-S) *slmb* MARCM clones (GFP positive) grow larger than WT clones but are strongly reduced when $aPKC^{DN}$ is expressed. $aPKC^{DN}$ alone does not affect growth or survival. Scale bars: 10 μm in A,L; 100 μm in D,O,P; 400 μm in H.

Tepass, 2003); the resulting morphogenetic defects are dependent on aPKC (Fig. 4J). Although heterozygosity for *slmb* does not enhance endocytic or Scrib module phenotypes, it does robustly enhance Crb overexpression (Fig. 4K). Finally, elevated aPKC activity is sufficient to induce trafficking defects of the retromer-dependent transmembrane cargo Wntless (Eaton, 2008), leading to a distinctive subcortical trapping phenotype (Fig. 4L,N; plasma membrane localization, 73±12% for WT versus 52±13% for $aPKC^{Act}$) (de Vreede et al., 2014); *slmb* mutant tissue phenocopies this trapping (Fig. 4M; plasma membrane localization, 44±25%; $P<2\times10^{-5}$ versus WT, $P=0.14$ versus $aPKC^{Act}$).

To directly test the functional involvement of hyperactive aPKC, we reduced aPKC activity in *slmb* cells using a weak dominant-negative construct ($aPKC^{DN}$) that has no effect on WT cells but can suppress phenotypes driven by elevated aPKC activity (Sotillos et al., 2004). Strikingly, expression of $aPKC^{DN}$ in *slmb* clones strongly suppressed tumorous growth (Fig. 4P-S). The resultant clones were smaller than WT clones, suggesting that aPKC activity also promotes *slmb* survival in this context, perhaps because tumorous *slmb* cells are 'addicted' to oncogenic aPKC, the excess activity of which allows them to survive in the presence of other misregulated *slmb* substrates. This reliance demonstrates a specific requirement for aPKC in *slmb* tissue and, along with the above results, reveal that Slmb acts as a negative regulator of aPKC activity.

Conclusions

Here, we extend the mechanisms involved in epithelial polarity to include a new function: targeted protein degradation. Targeted degradation can create spatial asymmetries in protein distributions, and there is precedent for roles of E3 ubiquitin ligases, including SCF^{Slmb} (Li et al., 2014; Morais-de-Sá et al., 2013), in polarizing different aspects of cells. The involvement of Slmb in *Drosophila* apicobasal polarity has gone unnoticed due to the previous use of hypomorphic alleles. The strong alleles described here display potent expansion of the apical pole of imaginal epithelia, demonstrating that Slmb is a new polarity regulator that functions to restrict the apical domain.

Loss of Slmb phenocopies the polarity defects associated with mutations in two classes of 'apical antagonists': the Scrib module of core polarity regulators, and endocytic regulators that control trafficking through the early endosome. Despite the similar polarity defects, *slmb* mutations do not alter endolysosomal cargo traffic, nor do they display protein recruitment defects characteristic of Scrib module mutants; furthermore, no genetic interactions are seen with either pathway. Nevertheless, the downstream consequences of polarity misregulation – including tumor-like transformation and the upregulation of specific target genes – are again shared between *slmb* and the other apical antagonists, and, moreover, *slmb* and Scrib module mutant cells share a distinctive trafficking defect associated

Development (2014) 141, 2978-2983 doi:10.1242/dev.109694

with elevated aPKC activity. We therefore suggest that Slmb acts in parallel to the Scrib module to antagonize the Par complex and other apical regulators.

The role for Slmb defined here points to the existence of an apical polarity-regulating protein substrate, the levels of which must be controlled. We have ruled out a number of validated Slmb substrates as the relevant target. Bioinformatic scans of *Drosophila* proteins for Slmb degron sequences suggest other candidates, including Expanded (Ex), but overexpression of Ex is not sufficient to induce polarity defects resembling those of *slmb* (Blaumueller and Mlodzik, 2000; Fernández et al., 2011). Although we cannot rule out a contribution from the elevation of multiple substrates, *slmb*-like polarity phenotypes can be induced by the elevated activity of individual proteins, including Crb or aPKC. Despite evidence that aPKC undergoes ubiquitin-mediated degradation in embryos (Colosimo et al., 2009), neither aPKC nor Crb levels appear to be controlled by Slmb-mediated degradation in imaginal discs. Nevertheless, our data together suggest that the substrate of Slmb in polarity regulation will function as a positive regulator of aPKC-driven outcomes.

Our demonstration that Slmb limits aPKC activity to distinguish the epithelial basolateral domain reveals intriguing parallels to polarization of the worm zygote. In this context, Par-2 is the primary antagonist that restricts aPKC/Par activity, while Lgl homologs function in a parallel, redundant role. Par-2 contains a RING finger domain that is characteristic of single-subunit E3 ligases, but Par-2 homologs have not been identified outside of nematodes, Par-2 does not affect aPKC/Par levels, and a degraded substrate in polarity regulation has yet to be identified (St Johnston and Ahringer, 2010; Zonies et al., 2010). The discovery of a *Drosophila* E3 ligase with a similar function to Par-2 raises the possibility of a conserved molecular logic to polarity in these two paradigmatic systems; determination of the relevant substrate will shed further light on this question.

MATERIALS AND METHODS

Fly stocks and genetics

Predominantly mutant imaginal discs were generated as described previously (Menut et al., 2007). *slmb* mutant images represent $slmb^{UU11}$ unless otherwise specified. For further details of fly stocks and genetics and the generation of mutants and clones, see supplementary Materials and Methods.

Immunohistochemistry and microscopy

Western blots loaded with equivalent protein concentrations were probed with anti-β-tubulin (E7, Developmental Studies Hybridoma Bank) and anti-aPKC (sc-216, Santa Cruz Biotechnology). Two biological replicates for each of six WT and four mutant technical replicates were quantitated.

Wandering L3 imaginal discs, larval CNS and ovaries were dissected in PBS on ice, fixed in 4% formaldehyde in PBS for 20 min at room temperature and stained using standard procedures (Bilder and Perrimon, 2000). Primary and secondary antibodies and stains are described in the supplementary Materials and Methods. Fluorescent tissues were mounted in SlowFade (Molecular Probes). Images are single sections taken with Leica TCS or Zeiss 700 confocal microscopes except for adult heads, which were frozen, mounted in agar and photographed using a Leica Z16 APO microscope and DFC300 FX camera. Images were assembled with Adobe Photoshop or Illustrator. Image quantitation used Fiji (Schindelin et al., 2012): cortical fluorescence intensity plots measured gray values along single-cell tracings; Wls cortical localization measured correlation coefficients with phalloidin staining.

Acknowledgements

We thank E. Knust, X. Lin, B. Lu and G. Bosco for providing reagents; N. Rusan for unpublished fly lines; S. Siegrist for shared expertise; X. Li for excellent technical assistance; and the D.B. lab for manuscript comments.

Competing interests

The authors declare no competing financial interests.

Author contributions

L.C.S., S.L.W. and D.B. designed the research; L.C.S., G.d.V., G.C.R. and S.L.W. performed the experiments; L.C.S., G.d.V., S.L.W., G.C.R. and D.B. analyzed the data; L.C.S., G.d.V., S.L.W. and D.B. wrote the manuscript.

Funding

This project was supported by grants from the National Institutes of Health [GM090150 and GM068675], the American Cancer Society [RSG-07-040-01-CSM] and a Burroughs Wellcome Fund Career Development Award to D.B. G.C.R. is grateful for support from the National Cancer Institute [P30 CA23074] and the Arizona Biomedical Research Commission [1210]. L.C.S. was the Robert Black Family Fellow of the Damon-Runyon Cancer Research Foundation [DRG2057-10]. Deposited in PMC for release after 12 months.

Supplementary material

Supplementary material available online at
http://dev.biologists.org/lookup/suppl/doi:10.1242/dev.109694/-/DC1

References

Bilder, D. (2004). Epithelial polarity and proliferation control: links from the Drosophila neoplastic tumor suppressors. *Genes Dev.* **18**, 1909-1925.

Bilder, D., Li, M. and Perrimon, N. (2000). Cooperative regulation of cell polarity and growth by Drosophila tumor suppressors. *Science* **289**, 113-116.

Blaumueller, C. M. and Mlodzik, M. (2000). The Drosophila tumor suppressor expanded regulates growth, apoptosis, and patterning during development. *Mech. Dev.* **92**, 251-262.

Buster, D. W., Daniel, S. G., Nguyen, H. Q., Windler, S. L., Skwarek, L. C., Peterson, M., Roberts, M., Meserve, J. H., Hartl, T., Klebba, J. E. et al. (2013). SCFSlimb ubiquitin ligase suppresses condensin II-mediated nuclear reorganization by degrading Cap-H2. *J. Cell Biol.* **201**, 49-63.

Chartier, F. J.-M., Hardy, É. J.-L. and Laprise, P. (2011). Crumbs controls epithelial integrity by inhibiting Rac1 and PI3K. *J. Cell Sci.* **124**, 3393-3398.

Colosimo, P. F., Liu, X., Kaplan, N. A. and Tolwinski, N. S. (2009). GSK3β affects apical-basal polarity and cell-cell adhesion by regulating aPKC levels. *Dev. Dyn.* **239**, 115-125.

de Vreede, G., Schoenfeld, J. D., Windler, S. L., Morrison, H., Lu, H. and Bilder, D. (2014). The Scribble module regulates retromer-dependent endocytic trafficking during epithelial polarization. *Development* **141**, 2796-2802.

Doggett, K., Grusche, F. A., Richardson, H. E. and Brumby, A. M. (2011). Loss of the Drosophila cell polarity regulator Scribbled promotes epithelial tissue overgrowth and cooperation with oncogenic Ras-Raf through impaired Hippo pathway signaling. *BMC Dev. Biol.* **11**, 57.

Eaton, S. (2008). Retromer retrieves Wntless. *Dev. Cell* **14**, 4-6.

Eder, A. M., Sui, X., Rosen, D. G., Nolden, L. K., Cheng, K. W., Lahad, J. P., Kango-Singh, M., Lu, K. H., Warneke, C. L., Atkinson, E. N. et al. (2005). Atypical PKCiota contributes to poor prognosis through loss of apical-basal polarity and cyclin E overexpression in ovarian cancer. *Proc. Natl. Acad. Sci. USA* **102**, 12519-12524.

Elsum, I., Yates, L., Humbert, P. O. and Richardson, H. E. (2012). The Scribble-Dlg-Lgl polarity module in development and cancer: from flies to man. *Essays Biochem.* **53**, 141-168.

Fernández, B. G., Gaspar, P., Brás-Pereira, C., Jezowska, B., Rebelo, S. R. and Janody, F. (2011). Actin-Capping Protein and the Hippo pathway regulate F-actin and tissue growth in Drosophila. *Development* **138**, 2337-2346.

Frescas, D. and Pagano, M. (2008). Deregulated proteolysis by the F-box proteins SKP2 and beta-TrCP: tipping the scales of cancer. *Nat. Rev. Cancer* **8**, 438-449.

Goldstein, B. and Macara, I. G. (2007). The PAR proteins: fundamental players in animal cell polarization. *Dev. Cell* **13**, 609-622.

Haack, T., Bergstralh, D. T. and St Johnston, D. (2013). Damage to the Drosophila follicle cell epithelium produces "false clones" with apparent polarity phenotypes. *Biol. Open* **2**, 1313-1320.

Halbsgut, N., Linnemannstöns, K., Zimmermann, L. I. and Wodarz, A. (2011). Apical-basal polarity in Drosophila neuroblasts is independent of vesicular trafficking. *Mol. Biol. Cell* **22**, 4373-4379.

Jiang, J. and Struhl, G. (1998). Regulation of the Hedgehog and Wingless signalling pathways by the F-box/WD40-repeat protein Slimb. *Nature* **391**, 493-496.

Laprise, P. and Tepass, U. (2011). Novel insights into epithelial polarity proteins in Drosophila. *Trends Cell Biol.* **21**, 401-408.

Lee, S., Wang, J.-W., Yu, W. and Lu, B. (2012). Phospho-dependent ubiquitination and degradation of PAR-1 regulates synaptic morphology and tau-mediated Aβ toxicity in Drosophila. *Nat. Commun.* **3**, 1312.

Li, S., Wang, C., Sandanaraj, E., Aw, S. S. Y., Koe, C. T., Wong, J. J. L., Yu, F., Ang, B. T., Tang, C. and Wang, H. (2014). The SCF SlimbE3 ligase complex regulates asymmetric division to inhibit neuroblast overgrowth. *EMBO Rep.* **15**, 619-729.

Development (2014) 141, 2978-2983 doi:10.1242/dev.109694

Menut, L., Vaccari, T., Dionne, H., Hill, J., Wu, G. and Bilder, D. (2007). A mosaic genetic screen for Drosophila neoplastic tumor suppressor genes based on defective pupation. *Genetics* **177**, 1667.

Milétich, I. and Limbourg-Bouchon, B. (2000). Drosophila null slimb clones transiently deregulate Hedgehog-independent transcription of wingless in all limb discs, and induce decapentaplegic transcription linked to imaginal disc regeneration. *Mech. Dev.* **93**, 15-26.

Morais-de-Sá, E., Vega-Rioja, A., Trovisco, V. and St Johnston, D. (2013). Oskar is targeted for degradation by the sequential action of Par-1, GSK-3, and the SCF-slimb ubiquitin ligase. *Dev. Cell* **26**, 303-314.

Morrison, H. A., Dionne, H., Rusten, T. E., Brech, A., Fisher, W. W., Pfeiffer, B. D., Celniker, S. E., Stenmark, H. and Bilder, D. (2008). Regulation of early endosomal entry by the Drosophila tumor suppressors Rabenosyn and Vps45. *Mol. Biol. Cell* **19**, 4167-4176.

Noureddine, M. A., Donaldson, T. D., Thacker, S. A. and Duronio, R. J. (2002). Drosophila Roc1a encodes a RING-H2 protein with a unique function in processing the Hh signal transducer Ci by the SCF E3 ubiquitin ligase. *Dev. Cell* **2**, 757-770.

Partanen, J. I., Tervonen, T. A. and Klefström, J. (2013). Breaking the epithelial polarity barrier in cancer: the strange case of LKB1/PAR-4. *Philos. Trans. R. Soc. Lond. B Biol. Sci.* **368**, 20130111.

Robinson, B. S. and Moberg, K. H. (2011). Drosophila endocytic neoplastic tumor suppressor genes regulate Sav/Wts/Hpo signaling and the c-Jun N-terminal kinase pathway. *Cell Cycle* **10**, 4110-4118.

Rogers, G. C., Rusan, N. M., Roberts, D. M., Peifer, M. and Rogers, S. L. (2009). The SCF Slimb ubiquitin ligase regulates Plk4/Sak levels to block centriole reduplication. *J. Cell Biol.* **184**, 225-239.

Schindelin, J., Arganda-Carreras, I., Frise, E., Kaynig, V., Longair, M., Pietzsch, T., Preibisch, S., Rueden, C., Saalfeld, S., Schmid, B. et al. (2012). Fiji: an open-source platform for biological-image analysis. *Nat. Methods* **9**, 676-682.

Shivas, J. M., Morrison, H. A., Bilder, D. and Skop, A. R. (2010). Polarity and endocytosis: reciprocal regulation. *Trends Cell Biol.* **20**, 445-452.

Sotillos, S., Díaz-Meco, M. T., Caminero, E., Moscat, J. and Campuzano, S. (2004). DaPKC-dependent phosphorylation of Crumbs is required for epithelial cell polarity in Drosophila. *J. Cell Biol.* **166**, 549-557.

St Johnston, D. and Ahringer, J. (2010). Cell polarity in eggs and epithelia: parallels and diversity. *Cell* **141**, 757-774.

Sun, G. and Irvine, K. D. (2011). Regulation of Hippo signaling by Jun kinase signaling during compensatory cell proliferation and regeneration, and in neoplastic tumors. *Dev. Biol.* **350**, 139-151.

Tanentzapf, G. and Tepass, U. (2003). Interactions between the crumbs, lethal giant larvae and bazooka pathways in epithelial polarization. *Nat. Cell Biol.* **5**, 46-52.

Tepass, U. (2012). The apical polarity protein network in Drosophila epithelial cells: regulation of polarity, junctions, morphogenesis, cell growth, and survival. *Annu. Rev. Cell Dev. Biol.* **28**, 655-685.

Theodosiou, N. A., Zhang, S., Wang, W. Y. and Xu, T. (1998). slimb coordinates wg and dpp expression in the dorsal-ventral and anterior-posterior axes during limb development. *Development* **125**, 3411-3416.

Windler, S. L. and Bilder, D. (2010). Endocytic internalization routes required for Delta/Notch signaling. *Curr. Biol.* **20**, 538-543.

Zonies, S., Motegi, F., Hao, Y. and Seydoux, G. (2010). Symmetry breaking and polarization of the C. elegans zygote by the polarity protein PAR-2. *Development* **137**, 1669-1677.

SUPPLEMENTARY MATERIALS AND METHODS

Fly stocks and genetics

Mutants used included *slmb*^{1}, *slmb*^{2}, *slmb*^{8}, *dlg*$^{40\text{-}2}$, *Roc1a*^{G1}, *AP-2sigma* and *yki*^{B5} (described in FlyBase). Transgenes included *tub>slmb-myc* (Ko et al., 2002), *UAS-Ci*$^{M1\text{-}4}$ (Chen et al., 1999), *UAS-Arm*^{S10} (Pai et al., 1997), *UAS-Plk4*^{SBM} (Rogers et al., 2009), *UAS-CapH2*^{SBM} (Buster et al., 2013), *UAS-Par1*^{T408A} (Lee et al., 2012), *UAS-aPKC*$^{CAAX\text{-}DN}$ (Sotillos et al., 2004) and *UAS-aPKC*$^{\delta N}$ (Betschinger et al., 2003) driven by *MS1096-GAL4*, as well as *hs-Wls-V5* and *UAS-Wls-V5* (Belenkaya et al., 2008). Entirely mutant wing discs were generated using *UbxFLP/FM7; cl FRT82B/TM6B* and entirely mutant eye discs were generated using *eyFLP cl GMRhid FRT82B/TM6B*. MARCM clones in the eye and neuroblast were generated with *eyFLP* and *hsFLP* stocks, respectively. Follicle cell clones were generated as described (Lu and Bilder, 2005).

Immunohistochemistry

The following primary antibodies were used: mouse anti-Mmp1 (1/100), mouse anti-Arm (N27A1, 1/100), mouse anti-Dlg (4F3, 1/100), mouse anti-Coracle (1/100), mouse anti-FasIII (7G10, 1/20), mouse anti-Notch^{ECD} (C458.2H, 1/50), mouse anti-Lamin (1/100), rat anti-Elav (9F8A9, 1/50) (all from Developmental Studies Hybridoma Bank, see references therein), rat anti-Crb (1/750; U. Tepass, E. Knust), guinea pig anti-Cad87E (1/1000; U. Tepass), guinea pig anti-Scrib (1/200), rabbit anti-PKCζ (sc-216, Santa Cruz Biotechnology, 1/200), rabbit anti-Miranda (1/500), mouse anti-Prospero (1/100). TRITC-phalloidin was used to visualize F-actin (1/400, Sigma) and either TO-PRO-3 (1/400) or DAPI (1/3000) was used to visualize DNA. Secondary antibodies were from Molecular Probes.

Supplementary references

Belenkaya, T. Y., Wu, Y., Tang, X., Zhou, B., Cheng, L., Sharma, Y. V., Yan, D., Selva, E. M. and Lin, X. (2008). The retromer complex influences Wnt secretion by recycling wntless from endosomes to the trans-Golgi network. *Dev Cell* **14**, 120–131.

Betschinger, J., Mechtler, K. and Knoblich, J. A. (2003). The Par complex directs asymmetric cell division by phosphorylating the cytoskeletal protein Lgl. *Nature* **422**, 326–330.

Buster, D. W., Daniel, S. G., Nguyen, H. Q., Windler, S. L., Skwarek, L. C., Peterson, M., Roberts, M., Meserve, J. H., Hartl, T., Klebba, J. E., et al. (2013). SCFSlimb ubiquitin ligase suppresses condensin II-mediated nuclear reorganization by degrading Cap-H2. *J. Cell Biol.* **201**, 49–63.

Chen, Y., Cardinaux, J. R., Goodman, R. H. and Smolik, S. M. (1999). Mutants of cubitus interruptus that are independent of PKA regulation are independent of hedgehog signaling. *Development* **126**, 3607–3616.

Ko, H. W., Jiang, J. and Edery, I. (2002). Role for Slimb in the degradation of Drosophila Period protein phosphorylated by Doubletime. *Nature* **420**, 673–678.

Lee, S., Wang, J.-W., Yu, W. and Lu, B. (2012). Phospho-dependent ubiquitination and degradation of PAR-1 regulates synaptic morphology and tau-mediated Aβ toxicity in Drosophila. *Nature Communications* **3**, 1312–12.

Lu, H. and Bilder, D. (2005). Endocytic control of epithelial polarity and proliferation in Drosophila. *Nat. Cell Biol.* **7**, 1232–1239.

Pai, L. M., Orsulic, S., Bejsovec, A. and Peifer, M. (1997). Negative regulation of Armadillo, a Wingless effector in Drosophila. *Development* **124**, 2255–2266.

Rogers, G. C., Rusan, N. M., Roberts, D. M., Peifer, M. and Rogers, S. L. (2009). The SCF Slimb ubiquitin ligase regulates Plk4/Sak levels to block centriole reduplication. *J. Cell Biol.* **184**, 225–239.

Sotillos, S., Diaz-Meco, M. T., Caminero, E., Moscat, J. and Campuzano, S. (2004). DaPKC-dependent phosphorylation of Crumbs is required for epithelial cell polarity in Drosophila. *J. Cell Biol.* **166**, 549–557.

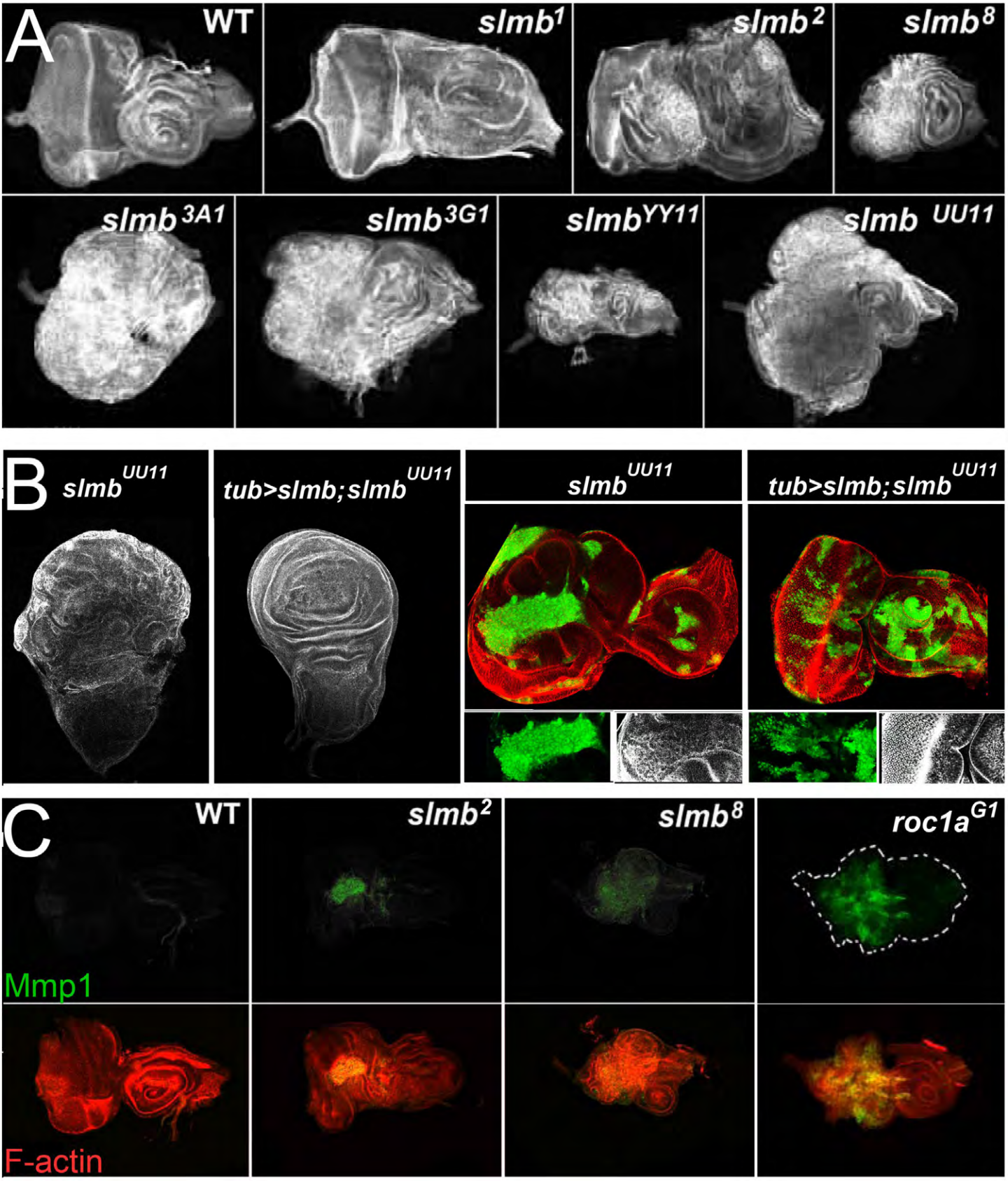

Supplementary Figure 1. Analysis of *slmb* allelic series. (**A**) Phalloidin staining of *slmb* mutant eye discs demonstrates that strong alleles show the most severe neoplastic transformation. (**B**) A *slmb* transgene rescues the neoplastic phenotypes of *UU11* in predominantly mutant wing discs and GFP-marked eye disc mosaics. (**C**) Discs derived from the deletion allele *slmb*^{8} and null mutation in the SCF core component *roc1a* also display hallmarks of neoplasia, including disrupted F-Actin and upregulation of Mmp1.

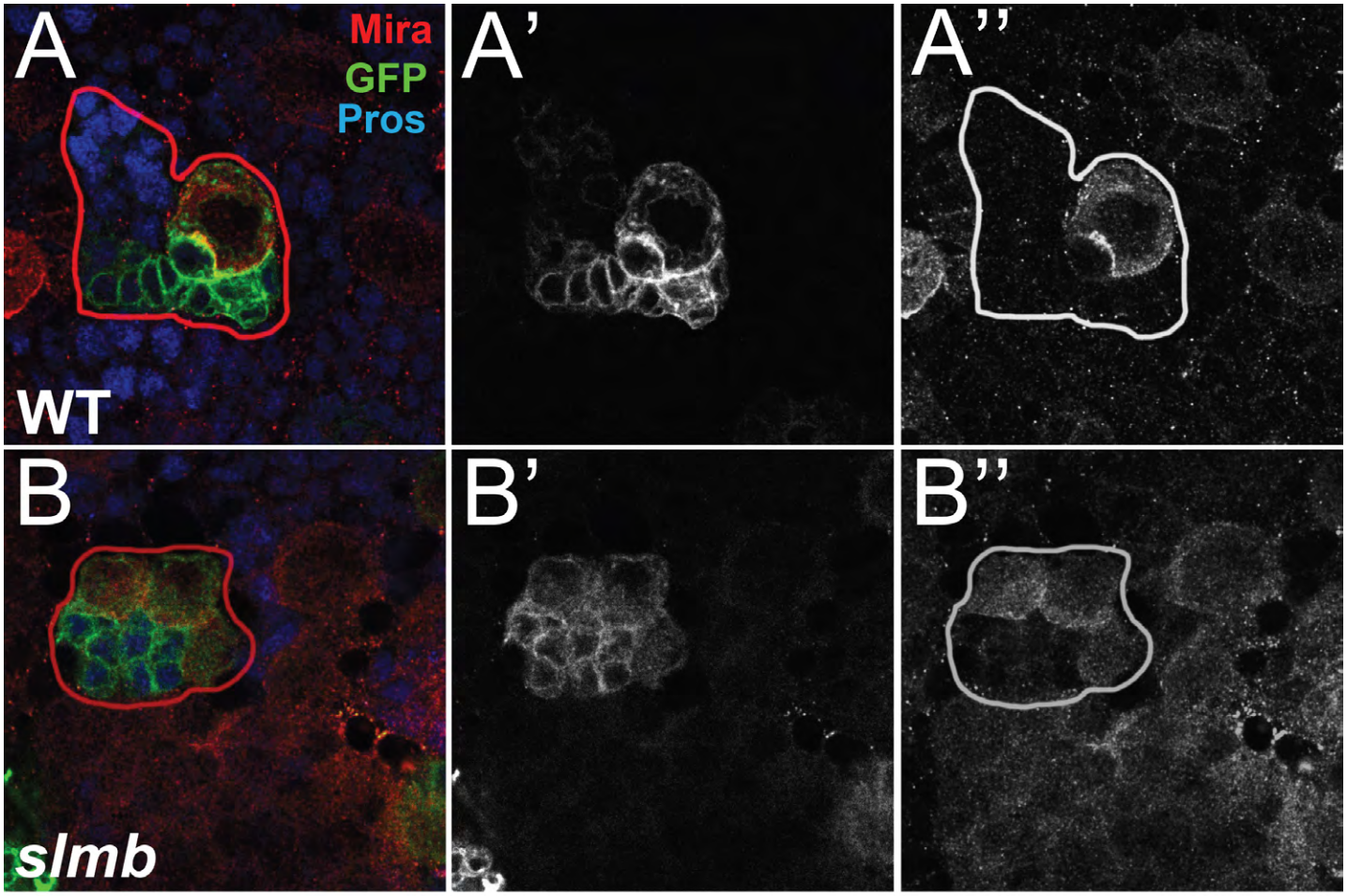

Supplementary Figure 2. Effect of loss of *slmb* in neuroblasts. (**A, B**) GFP marks clones generated using the MARCM system. Larval type I neuroblasts divide asymmetrically to produce a new Miranda-positive neuroblast (red) and a smaller ganglion mother cell that will differentiate into a neuron or glia (Prospero positive, blue). *slmb* mutant neuroblasts display defects in asymmetric cell division, with a fraction of clones containing multiple Miranda positive neuroblast-like cells.

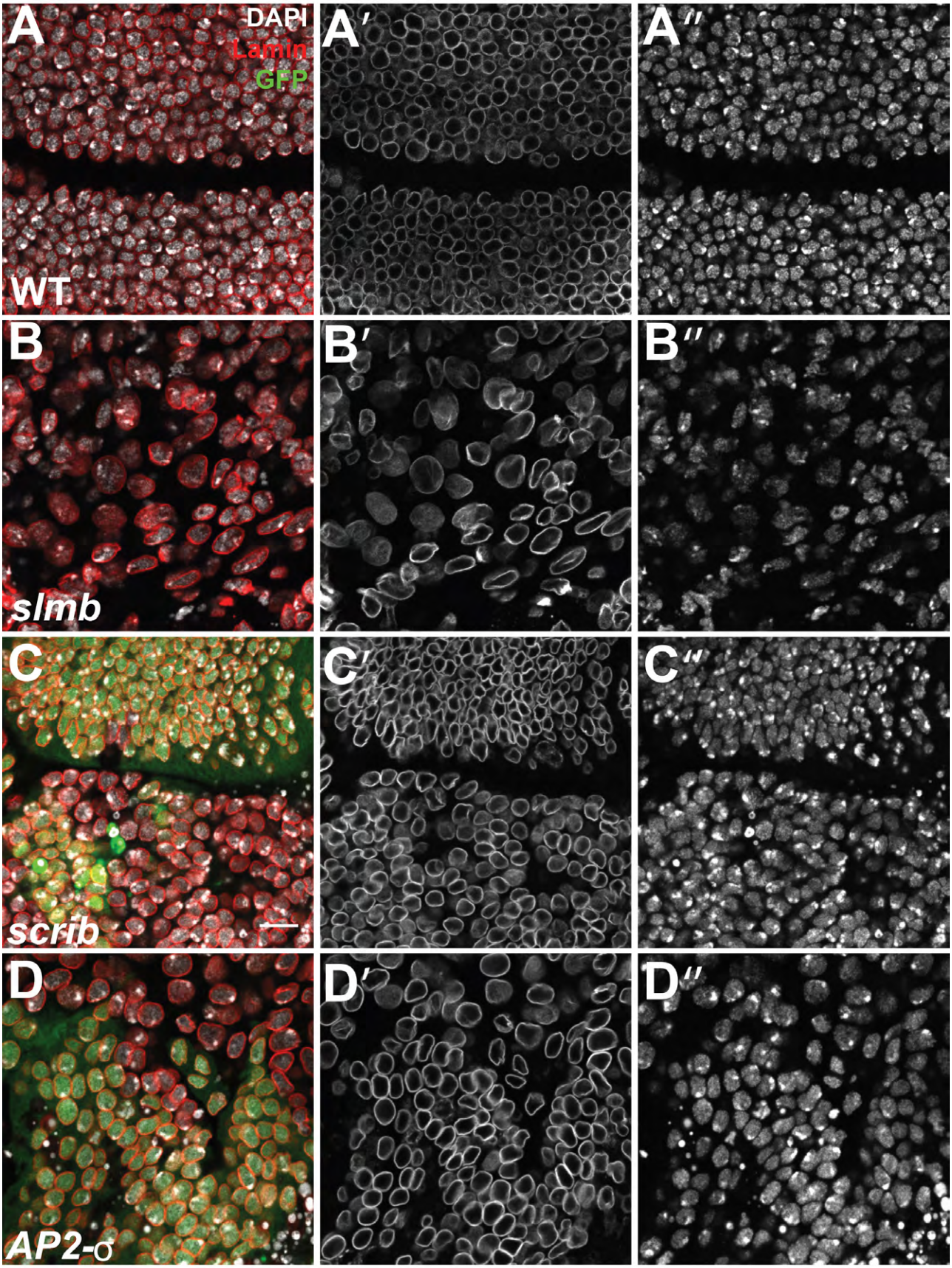

Supplementary Figure 3. Junctional scaffold and endocytic class tumor suppressors do not regulate Slmb activity. (**A, B**) Cells mutant for strong *slmb* alleles show chromosome condensation defects leading to a swollen nuclear lamina, reflecting misregulation of Condensin components. (**C,D**) In contrast, *scrib* and *AP2-sigma* mutant cells have WT nuclei and lamina size. Presence of GFP marks mutant cells. Scale, 10 mm.

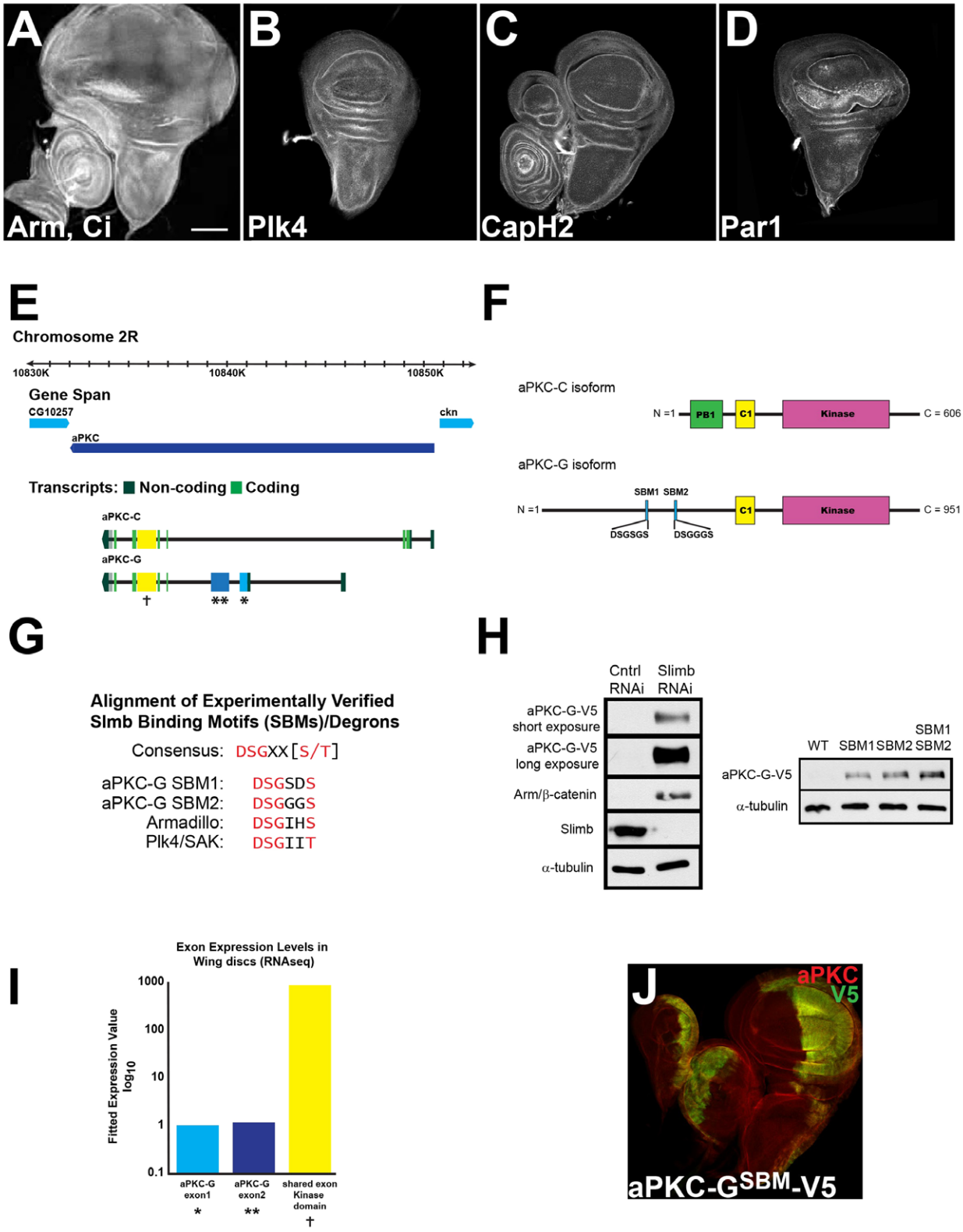

Supplementary Figure 4. Misregulation of known substrates cannot account for the *slmb* phenotype. (**A-D**) Overexpression of stabilized versions of known Slmb substrates throughout the presumptive wing pouch and notum using *MS-1096GAL4* does not phenocopy loss of *slmb*. (**E, F**) Gene and protein models comparing a common aPKC isoform C with the G isoform containing two Slmb binding motifs (SBM). (**G**) Alignment of aPKC-G SBMs with experimentally validated SBM degrons from other Slmb targets. (**H**) Western blots demonstrating that RNAi mediated knockdown of *slmb* in S2 cells results in stabilization of the aPKC-G isoform, as does mutation of the SBMs. (**I**) RNAseq data from third instar wing discs comparing levels of the unique aPKC-G exons with an exon encoding the shared Kinase domain; values shown are derived from RPKM. (**J**) Overexpression of a stabilized version of aPKC-G in the posterior domain of the wing disc (*en>GFP*, green) does not affect polarity or growth.